

Schwan equation and transmembrane potential induced by alternating electric field

Piotr Marszalek, D.-S Liu, and Tian Y. Tsong

Department of Biochemistry, University of Minnesota College of Biological Sciences, St. Paul, Minnesota 55108 USA

ABSTRACT The transmembrane potential generated by an alternating electric field (ac) depends strongly on the frequency of the field and can be calculated using the Schwan Equation. We have measured the critical electric breakdown potential, $\Delta\psi_{crit}$, of the plasma membrane of murine myeloma cell line (Tib9) using ac fields, by monitoring the entry of a fluorescence probe, propidium iodide, into the cells. This dye is weakly fluorescent in solution but becomes strongly fluorescent when it binds to DNA. Experiments were done under a microscope by direct visual examination of single cells or by examining photographic prints. When an ac field reached the intensity, E_{crit} , that generated a maximal membrane potential $\Delta\psi_{max}$, equal to or greater than the $\Delta\psi_{crit}$, the membrane was perforated at the two loci facing the electrodes. The dye diffused into the cell, giving rise to two bright, narrow bands, which expanded to the whole cell in 1–3 min. $\Delta\psi_{crit}$'s were measured in three media of different resistivities, ρ_{ext} , (52,600, 7,050, and 2,380 Ω cm), over the range of 0.1–300 kHz, with the field duration of 200 ms. Regression analysis based on the Schwan Equation showed that in a medium of given resistivity, the $\Delta\psi_{crit}$ was constant over the frequency range studied. When the capacitance of the membrane, C_{membr} , was taken to be 0.90 μ F cm⁻², the resistivity of the cytoplasmic medium, ρ_{int} , was determined to be 910–1,100 Ω cm. The $\Delta\psi_{crit}$ were 0.33, 0.48, and 0.53 V, respectively, for the three media in decreasing resistivities. The good fit of these data to the curves calculated using the Schwan Equation indicates that the equation may be used to describe the transmembrane potential of a living cell generated by an oscillating electric field.

INTRODUCTION

Electroporation and electrofusion of cell membranes have been known for many years (1–9). These methods have now been applied to molecular biology for DNA transfection of cells (9, 10) and electroinsertion of biologically active molecules into cell membranes (11); to immunochemistry, for the preparation of monoclonal antibodies (12); to agriculture research, for fusing plant cells or protoplasts (9) etc. Electroactivation of membrane enzymes (13) and electrostimulation of cellular functions (14) are other areas of current interest. In these experiments, different waveforms of electric fields are applied to cells or organelles in suspension or in monolayer culture, or to a piece of tissue, or to organisms confined in a chamber. There is ample experimental evidence which shows that these effects of an electric field result from the field-induced electric potential across the cell membranes (13–26). A direct experimental measurement of a field-induced transmembrane potential, $\Delta\psi_{membr}$, requires sophisticated instrumentations and is not practical for most cell biology laboratories. Some simple relationships de-

rived from electromagnetic theory have frequently been used to calculate $\Delta\psi_{membr}$ from the applied field, E_{appl} .

For a cell (of outer radius a and inner radius b), suspended in a physiological medium, the transmembrane potential generated by an applied dc field may be calculated according the maxwell relationship (see reference 13 and references cited therein),

$$\Delta\psi_{membr} = 1.5aE_{appl} \cos \theta. \quad (1)$$

In the Eq. 1, E_{appl} is the applied field strength in volts per centimeter and θ is the angle between the field line and a normal from the center of the sphere to a point of interest on the cell membrane. The conditions for Eq. 1 to be valid are the following: a cell of the spherical shape, a much higher resistivity of the membrane than those of the internal and the external media, and a thin membrane compared with the radius of the cell. Relationships for cells of spheroid shape have also been derived (17, 20, 25). In Eq. 1, when $\theta = 0^\circ$ or 180° , $|\cos \theta| = 1$. Thus, the maximal transmembrane potential, $\Delta\psi_{max}$, which occurs at the two loci facing the electrode is

$$\Delta\psi_{max} = 1.5aE_{appl}. \quad (2)$$

Eqs. 1 and 2 have been shown to be applicable to lipid vesicles and cell membrane by two types of experiments.

Address correspondence to Dr. Tsong.

Dr. Marszalek is Junior Fulbright Fellow from the Institute of Electrotechnical Research, Warsaw, Poland.

The first type uses potential sensitive fluorescence dyes to image the field-induced transmembrane potential (17–19). The second type measures entrance or leakage of fluorescence probes or radioactive tracers at the critical breakdown potential, $\Delta\psi_{\text{crit}}$, of lipid vesicles of a narrow size distribution and compares the value obtained with planar lipid bilayer (21, 26). These experiments indicate that Eqs. 1 and 2 are applicable to lipid bilayers and to cell membranes.

However, when an ac field is used, the situation becomes more complex. In this case, the induced transmembrane potential becomes strongly dependent on the frequency of the applied field when the frequency approaches the relaxation time, τ , of the membrane. Schwan (27) has derived a relationship from the basic electromagnetic theory for calculation $\Delta\psi_{\text{membr}}$ induced by an oscillating electric field.

$$\Delta\psi_{\text{membr}} = 1.5 a E_{\text{appl}} \cos \theta / [1 + (\omega\tau)^2]^{1/2}, \quad (3)$$

where

$$\tau = a C_{\text{membr}} (\rho_{\text{int}} + \rho_{\text{ext}}/2). \quad (4)$$

In Eqs. 3 and 4, $\omega = 2\pi f$, and f is the frequency of the applied ac field. C_{membr} , ρ_{int} , and ρ_{ext} are, respectively, the capacitance of the membrane in F cm^{-2} , the resistivity of the internal fluid, and that of the external medium, both in $\Omega \text{ cm}$. The maximal transmembrane potential induced by an oscillating field of the form, $E_{\text{appl}} = E_{\text{appl}}^{\circ} \sin(\omega t)$, where E_{appl}° is the amplitude of the field and t is time, is,

$$\Delta\psi_{\text{max}} = 1.5 a E_{\text{appl}}^{\circ} / [1 + (\omega\tau)^2]^{1/2}. \quad (5)$$

The use of oscillating electric fields instead of dc electric pulses for electroporation, electrofusion, and electroactivation of the cell membrane has gained increasing popularity in recent years (see references 13–15 and references cited therein). The electrical parameters of a cell membrane would depend on the frequency of an ac field (13, 14, 27, 28). In this paper, we will use murine myeloma cell line Tib9 as a model system to study the breakdown potential of its membrane and to establish the relationship between $\Delta\psi_{\text{crit}}$ and the frequency of the applied ac field. The relationship relevant for these experiments would be

$$\Delta\psi_{\text{crit}} = 1.5 a E_{\text{crit}} / [1 + (\omega\tau)^2]^{1/2}. \quad (6)$$

MATERIALS AND METHODS

Instruments and cell poration chamber

A pulse generator (model 801; Wavetek San Diego, Inc., San Diego, CA) was used to trigger a Wavetek San Diego, Inc. model 148A ac

generator to produce an ac field of desired amplitude and frequency. The experimental chamber was made of a pair of parallel plate platinum electrodes glued to a glass microscope slide. The electrodes have a length of 15 mm, a width of 10 mm, and a height of 0.3 mm. The distance between the electrodes was 0.10 mm and they were circled with an epoxy ring to form a chamber of ~ 0.15 ml. The waveform, amplitude, and frequency of the ac field across the two electrodes were monitored directly with an oscilloscope (model 7704A; Tektronix Inc., Beaverton, OR). Contamination or distortion of the sinusoidal waveform of the ac field by the triggering pulse was insignificant. The conductivity of a cell suspension was measured by a conductometer (model 31A; Yellow Spring Instr. Co., Yellow Spring, OH) and was controlled during each experiment by measuring the chamber current with a generator signal of 3 V (peak-to-peak) at 1 kHz. A block diagram of the set up and the chamber design are given in Fig. 1.

Cells and sample preparations

Murine myeloma cell line Tib9 was obtained from American Tissue Culture Collections. Tib9 was chosen because of its spherical shape in suspension. Cells were grown in RPMI 1640 medium (Sigma Chemical Co., St. Louis, MO) supplemented with 10% fetal bovine serum, 2% L-glutamine, and 0.4% vol/vol gentamicin (10 mg/ml), at 37°C in 5% CO_2 . Cells were collected by centrifugation at 800 g for 5 min and suspended in a small amount of the original medium. Shortly before each measurement, an aliquot of cells was transferred into a 2-mM

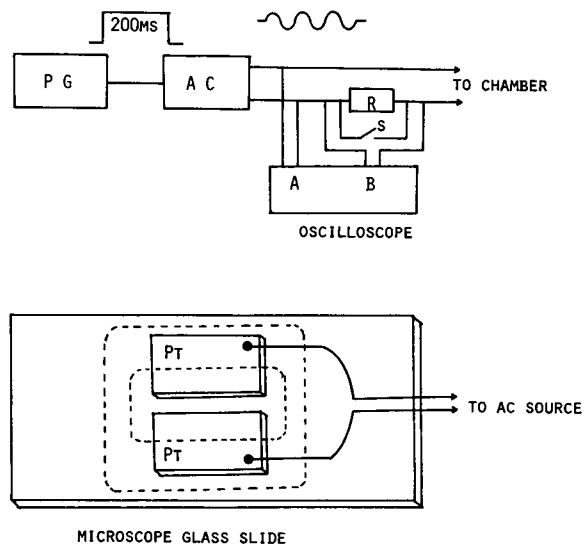


FIGURE 1 Block diagrams of equipment and cell chamber for electroporation. The upper figure is the block diagram of the equipment used for electroporation: PG denotes the pulse generator (model 801; Wavetek); AC, the functional generator (model 148A; Wavetek); R, a 47 Ω noninductive resistor; and S, a switch. The lower figure illustrates the cell chamber. An ac field of appropriate amplitude and frequency was generated by the functional generator and applied to the cell suspension. The duration of the ac field was 200 ms, and was controlled by a square wave triggering pulse. The distance between the two platinum electrodes was 0.1 mm. The dashed lines in the glass slide indicate the epoxy resin ring which formed a vessel to hold 150 μl of cell suspension. The conductivity of the cell suspension was monitored during the experiment by measuring the voltage drop on the noninductive 47 Ω resistor.

Na,K phosphate buffer at pH 7.2. In this case the resistivity of the suspension was $\sim 2,500 \Omega \text{ cm}$. In some experiments, cells were washed once more by the 2-mM Na,K phosphate buffer by centrifugation, and the resistivity of this suspension was $\sim 7,000 \Omega \text{ cm}$. To obtain high resistivity of a cell suspension, cells were washed by a 0.3-M sucrose solution and suspended in the sucrose solution. In this case, the resistivity was $\sim 50,000 \Omega \text{ cm}$. Cells were found to be unstable in this high resistivity medium and were used within 5–10 min. After 30 min electric parameters of these cells changed. In all experiments, uniformly spherical cells with the radius of $6.5 \pm 0.5 \mu\text{m}$ were chosen for measurements.

Electroporation experiment

Propidium iodide binds specifically to DNA and has been used as a marker of cell nuclei (29). Its excitation wavelength is 493 nm and emission wavelength is 639 nm. In our experiments, a green filter was used for the excitation beam and a red filter was used for the observation. Propidium iodide was added to a diluted cell suspension to the final concentration of $10 \mu\text{M}$. After a few min of incubation, the cell suspension was transferred to the electroporation chamber and the chamber current was measured. Electroporation was performed while the chamber slide was mounted on a fluorescence microscope (Carl Zeiss, Inc., Thornwood, NY) for a continual observation. In many cases, fluorescence stained dead cells were found before electroporation. These dead cells were discounted. A 200-ms sine wave ac pulse with a selected field strength and frequency was then applied to the suspension. If the field strength was too low, no changes would be observed. After a 3-min observation, the sample was discarded and replaced by a new sample which was examined using a higher field strength. The voltage increment for each step was typically 1 V (peak-to-peak), or 50 V/cm. When the field strength reached an intensity which could generate $\Delta\psi_{\text{memb}} \geq \Delta\psi_{\text{crit}}$, most cells became brighter within 3 s, at the two loci facing the electrodes (in the fluorescence mode). These cells were monitored carefully for several min and occasionally photographs were taken for permanent records. We rarely observed cells which brightened up only on one locus. The 200-ms pulse duration was chosen to ensure that even with the lowest frequency used (100 Hz), each ac pulse would contain many cycles (20 cycles) to be truly oscillatory. In these experiments the concentration of cells was very low. Typically only a few cells were visible in the microscope. This was to avoid cell aggregations due to the dielectrophoresis of the ac field (9, 30). Such phenomenon usually takes place at a much lower field strength.

Measurements of membrane capacitance, C_{memb} , followed the dielectrophoresis method described by Marszalek et al. (30). This method measures the dielectrophoretic spectrum of single cells. From the dependence of f_0 , the critical frequency in which a cell experiences not net forces, on the conductivity of the suspending medium, the dielectric constant of the cell membrane is determined (Marszalek, M., J. J. Zielinski, M. Fikus, and T. Y. Tsong, unpublished results). C_{memb} is the ratio of the dielectric constant and the thickness of the membrane (8 nm).

RESULTS AND ANALYSIS

Dependence of critical field strength on ac frequency

Some observations of a typical experiment are recorded in Fig. 2. A cell in the bright field is shown before electroporation and the positions of the two electrodes are indicated. When an ac field (1 kHz, 550 V/cm, 200 ms) was

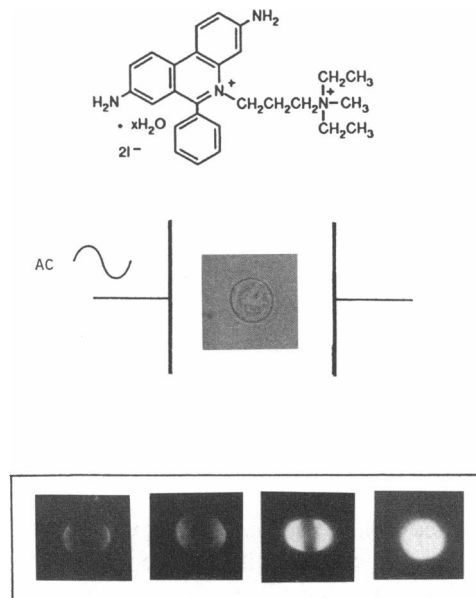


FIGURE 2 Observation of electroporation by the fluorescence changes of propidium iodide. The chemical formula of propidium iodide is given in the upper figure. The middle figure shows a typical myeloma cell under the microscope (bright field). The relative positions of the platinum electrodes are indicated. The lower figure gives some photographs taken at different time after a cell was electroporated by an ac field E_{crit} . Within 1–3 s, two narrow, bright bands appeared at the two loci facing the electrodes (the left most photo). The next 3 photos, from left to right, were taken at ~ 20 s, 1 min, and 3 min, respectively. See text for details.

applied, within 3 s the two edges close to the two electrodes became fluorescent. It is known that myeloma Tib9 has a large nucleus which occupies more than 90% of the cytoplasmic space. Thus, the DNA content of the cell permeates most of the cell volume. When the membrane of a cell was perforated by the ac field, propidium iodide (molecular weight 668.4) diffused into the cell through the regions where the normals paralleled the field lines, i.e., where θ of Eq. 3 was close to either 0° or 180° . For the regions where θ was close to either 90° or 270° no penetration of the fluorescence probe was evident. These observations indicate that the applied field was either equal to or only slightly greater than critical field strength, E_{crit} , for electroporation of the cell membrane and was accepted as the E_{crit} . After 20 s, the dye diffused to larger areas, and these areas continued to expand and eventually filled the cytoplasmic space in 1–3 min. In many occasions, a slight elongation of cells along the field lines was observed. This phenomenon was not investigated further. Application of Eqs. 2, 5, and 6 requires that the conductivity of the cytoplasmic fluid is much greater than that of the cell membrane. Myeloma Tib9 has a large nucleus and how such a nucleus affects the conductivity of the

TABLE 1 Some electric parameters of myeloma cells

Parameter	Experiment 1	Experiment 2	Experiment 3
a (μm)	6.5	6.5	6.5
ρ_{ext} (Ωcm)	52600	7050	2380
ρ_{int} (Ωcm)	n.a.	910	1100
α	0.17	0.030	0.015
τ' (μs)	13*	2.5†	1.3‡
$\Delta\psi_{crit}$ (V)	0.33	0.48	0.53
$\Delta\psi_{rms}$ (V)	0.23	0.34	0.37

n.a. means not applicable.

*Value obtained by calculation.

†Values obtained by optimization.

$\Delta\psi_{rms} = \Delta\psi_{crit}/\sqrt{2}$. These values are for the permeation of propidium iodide only. Use of other probes may give different values.

cellular space is not known. However, data in Table 1 indicate that the conductivity of the internal fluid was high and should have no effect on our interpretation.

The critical field strengths for electroporation in the media of three different resistivities (O for the medium of 52,600 Ωcm , ● for 7,050 Ωcm , and □ for 2,380 Ωcm), using ac fields of frequencies 0.1–300 kHz are shown in Fig. 3. In all three different conditions, the critical field strength for electroporation was strongly dependent on the frequency of the ac field. This dependence was nonlinear and was much more pronounced for frequencies >10 kHz. Experiments with a 1-ms square wave dc field gave a $\Delta\psi_{crit}$ of 0.95 V. Longer than 1 ms dc pulses were not used because these pulses can cause electrolysis.

Analysis based on the Schwan Equation

Data in Fig. 3 revealed several essential features. (a) At low frequencies [$f \ll (2\pi\tau)^{-1}$], the E_{crit} was independent of the ac frequency. Consequently, $\Delta\psi_{crit}$ would not depend on f . (b) At higher frequencies [$f \gg (2\pi\tau)^{-1}$], membrane polarization was reduced by the relaxation time, τ , of the membrane. Under these conditions, it would take a greater E_{appl} to generate the same $\Delta\psi_{crit}$. That, E_{crit} increased with increasing frequency. (c) As the ρ_{ext} increased, there was a corresponding increase of τ according to Eq. 4, and subsequently a shift in the position of curves in Fig. 3 toward the lower frequency.

To perform regression analysis using Eqs. 4 and 6, membrane capacitance, C_{membr} , must be determined by an independent method. The dielectrophoresis method (30) outlined in Materials and Methods was used to determine C_{membr} (0.90 $\mu F cm^{-2}$). In the analysis we assumed that $\Delta\psi_{crit}$ would not depend on the frequency. Regression analysis was performed to fit the data obtained with the media of 7,050 Ωcm (Fig. 3, data in ●) and 2,380 Ωcm

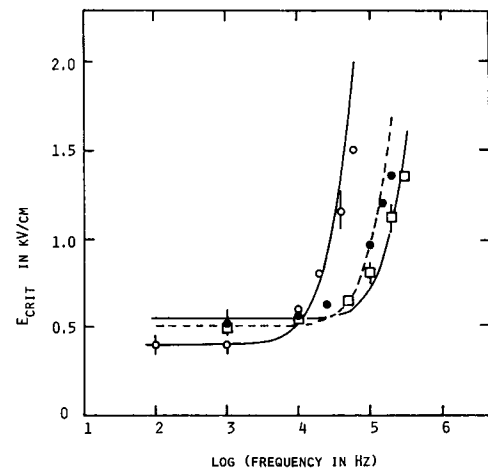


FIGURE 3 Critical ac field strength, E_{crit} , for electroporation as a function of the ac frequency. Data obtained in three media of different resistivities, 52,600 Ωcm (O), 7,050 Ωcm (●), and 2,380 Ωcm (□), are shown. The curves drawn through these data points were obtained by calculation (O) or the optimization (● and □) according to Eq. 6. These values of E_{crit} were for the permeation of propidium iodide only. Use of other probes may give different values. See text for details.

(Fig. 3, data in □) using Eq. 6. A good fit shown in Fig. 3 indicated that $\Delta\psi_{crit}$ was constant for the frequency range studied. The analysis also allowed us to determine ρ_{int} . Its values in the two media turned out to be ~1,000 Ωcm (Table 1). Other electric parameters of the myeloma, determined by these procedures, are also given in Table 1. For the data obtained in the medium of high resistivity (52,600 Ωcm), we simply ignored ρ_{int} in Eq. 4 and calculated E_{crit} as a function of frequency according to Eq. 6. As shown in Fig. 3 (data in O), the fit was also good.

One further note is in order. In our dielectrophoresis experiments, G_{membr} was also determined ($1 \times 10^{-2} \Omega^{-1} cm^{-2}$). This value appeared to be high and could not be ignored in the analysis of data obtained with the high resistivity medium (52,600 Ωcm). The Schwan Equation is applicable only if the conductivity of a cell membrane is much smaller than those of the cytoplasmic fluid and the external medium. When this is not true, a correction would be required. When the conductivity of the membrane approaches that of the external medium, Eq. 6 becomes

$$\Delta\psi_{crit} = \frac{1.5aE_{crit}}{1 + \alpha} \cdot \frac{1}{[1 + (\omega\tau')^2]^{1/2}} \quad (7)$$

$$\tau' = \tau/(1 + \alpha), \quad (8)$$

where

$$\alpha = G_{membr}a(\rho_{int} + \rho_{ext}/2). \quad (9)$$

If

$$\rho_{\text{int}} \ll \rho_{\text{ext}}$$

then

$$\alpha = aG_{\text{membr}}\rho_{\text{ext}}/2. \quad (10)$$

Eq. 10 was used to calculate α for the data obtained in the high resistivity medium (0.17). Regression analysis was then performed to determine α for the data obtained in the lower resistivity media. The results are given in Table 1 (regression curves not shown). The low values of α indicate that correction is not necessary to obtain E_{crit} when an experiment is done in a medium of low resistivity.

DISCUSSION

Fluorescence probe technique has been used to investigate different molecular events of electroporations and electrofusions of cell membranes. For example, the magnitude and the spacial distribution of the transmembrane potential induced by an electric pulse have been measured and analyzed using potential sensitive fluorescence dyes for a few types of cells and lipid vesicles (9, 17–19). Surface and content mixing of electrically fused cells, size distributions of pores, and electroosmosis effects have also been studied using fluorescence probe technique (9, 23, 31–34). We have used propidium iodide to measure $\Delta\psi_{\text{crit}}$ of myeloma cell line Tib9 induced by an oscillating electric field. Propidium iodide is relatively small (molecular weight 668.4), water soluble, and binds preferentially to DNA. When an applied field induced $\Delta\psi_{\text{membr}} = \Delta\psi_{\text{crit}}$, the cell membrane was perforated at the two loci facing the electrodes, i.e., at the areas where θ of Eq. 3 was either 0° or 180° . The dye permeated into the cell, bound to DNA and became strongly fluorescent. Several of our observations are significant. First, our results confirm that electroporation is a local phenomenon; a global breakdown of cell membranes did not occur (6–9). Second, a reasonably good fit for the ac electroporation data obtained in the three suspensions of different resistivity indicates that $\Delta\psi_{\text{crit}}$ was constant in the frequency range studied (0.1–300 kHz). Third, the $\Delta\psi_{\text{crit}}$ of the myeloma membrane with 200 ms ac field was low. The root mean square critical potential $\Delta\psi_{\text{rms}}$ for the membrane perforation was 0.23–0.37 V. Most experiments using square wave dc of durations in the range of microseconds to a few milliseconds found a $\Delta\psi_{\text{crit}}$ of ~ 1 V (9, 16, 22, 24, 25). Our measurements with a 1-ms square wave dc gave a $\Delta\psi_{\text{crit}}$ of 0.95 V. It is known that $\Delta\psi_{\text{crit}}$ depends strongly on the pulse duration (9, 25). The longer a dc pulse is the lower the $\Delta\psi_{\text{crit}}$ would be. However, a long dc pulse can

cause electrolysis of the solution, thus, giving rise to many side effects. Fourth, in our experiments the probability of electroporation at each of the two loci facing the electrodes was approximately equal no matter whether an ac or a dc field was used. Previous studies from several laboratories indicate asymmetric entry of dyes and calcium ions (31–33). These results have been explained by the electroosmosis effect of the applied field. In our ac experiments, any electroosmosis effect if existing at all would be symmetrical. However, we do not believe the dye entry in this case was driven by an electroosmosis effect. The ac pulse we used lasted only for 200 ms. Significant dye entry was observed only after the electric field was turned off (1 s to 3 min after electroporation). In other words, propidium iodide permeated into a cell in the absence of any applied electric field. The fact that in our experiment a dc pulse (1 ms) also consistently induced a symmetric entry of dye from the two poles facing the electrodes suggests that the myeloma cell line used in these experiments has a negligible natural, endogenous transmembrane potential. However, this point remains to be verified. And, finally, our results confirm that the Schwan Equation is satisfactory for describing an ac-induced transmembrane potential of a biological cell which is spherical.

We thank Dr. L. V. Chernomordik for suggesting the fluorescence probe, propidium iodide, and C. J. Gross for helping the manuscript.

This work was supported by a grant from the U.S. Office of Naval Research.

Received for publication 11 May 1990 and in final form 11 July 1990.

REFERENCES

1. Cole, K. C. 1971. *Membranes, Ions and Impulses*. University of California Press, Berkeley, CA. 569 pp.
2. Goldman, D. E. 1943. Potential impedance and rectification in membranes. *J. Gen. Physiol.* 27:37–50.
3. Coster, H. G. L. 1965. A quantitative analysis of the voltage-current relationships of fixed charge membranes and the associated property of "punch-through." *Biophys. J.* 5:669–686.
4. Huang, C.-H., L. Wheelodon, and T. E. Thompson. 1964. The properties of lipid bilayer membranes separating two aqueous phases: formation of a membrane of simple composition. *J. Mol. Biol.* 8:148–160.
5. Sale, A. J. H., and W. A. Hamilton. Effects of high fields on micro-organisms III. Lysis of erythrocytes and protoplasts. *Biochim. Biophys. Acta.* 163:37–43.
6. Kinosita, K., and T. Y. Tsong. 1977. Formation and resealing of pores of controlled sizes in human erythrocyte membrane. *Nature (Lond.)*. 268:438–441.
7. Sowers, A. E. 1985. Movement of a fluorescent lipid label from a labeled erythrocyte membrane to an unlabeled erythrocyte mem-

- brane following electric field-induced fusion. *Biophys. J.* 47:519–525.
8. Chang, D. C., and T. S. Reese. 1990. Changes of membrane structure induced by electroporation as revealed by rapid-freezing electron microscopy. *Biophys. J.* 58:1–12.
9. Neumann, E., A. E. Sowers, and C. A. Jordan. 1989. *Electroporation and Electrofusion in Cell Biology*. Plenum Press, New York, 436 pp.
10. Wong, T.-K., and E. Neumann. 1982. Electric field mediated gene transfer. *Biochem. Biophys. Res. Commun.* 107:584–587.
11. Mouneimne, Y., P.-F. Tosi, Y. Gazitt, and C. Nicolau. 1989. Electro-insertion of xeno-glycophorin into the red blood cell membrane. *Biochem. Biophys. Res. Commun.* 159:34–40.
12. Lo, M. M. S., T. Y. Tsong, M. K. Conrad, S. M. Strittmatter, L. D. Hester, and S. Snyder. 1984. Monoclonal antibody production by receptor-mediated electrically induced cell fusion. *Nature (Lond.)*. 310:792–794.
13. Tsong, T. Y. 1990. Electrical modulation of membrane proteins: enforced conformational oscillations for biological energy and signal transductions. *Annu. Rev. Biophys. Biophys. Chem.* 19:83–106.
14. Weaver, J., and R. D. Astumian. 1990. The response of living cells to very weak electric fields: the thermal noise limit. *Science (Wash. DC)*. 247:459–462.
15. Pliquett, F. 1983. Electrical field effects on a single cell. *Stud. Biophys.* 94:85–90.
16. Kinoshita, K., and T. Y. Tsong. 1977. Hemolysis of human erythrocytes by transient electric field. *Proc. Natl. Acad. Sci. USA*. 74:1923–1927.
17. Gross, D., L. M. Loew, and W. W. Webb. 1986. Optical imaging of cell membrane potential changes induced by applied electric fields. *Biophys. J.* 50:339–348.
18. Kinoshita, K., I. Ashikawa, N. Saita, H. Yoshimura, H. Itoh, K. Nagayama, and A. Ikegami. 1988. Electroporation of cell membrane visualized under a pulsed-laser fluorescence microscope. *Biophys. J.* 53:1015–1019.
19. Ehrenberg, B., D. L. Farkas, E. N. Fluhler, Z. Lujewska, and L. M. Loew. 1987. Membrane potential induced by external electric pulse can be followed with a potentiometric dye. *Biophys. J.* 51:833–837.
20. Bernhardt, J., and H. Pauly. 1973. On the generation of potential difference across the membranes of ellipsoidal cells in an alternating electric field. *Biophysik*. 10:89–98.
21. Teissie, J., and T. Y. Tsong. 1981. Electric field induced transient pores in phospholipid bilayer vesicles. *Biochemistry*. 20:1548–1554.
22. Sowers, A. E., and M. L. Lieber. 1986. Electropores in individual erythrocyte ghosts: diameters, lifetimes, numbers, and locations. *FEBS (Fed. Eur. Biochem. Soc.) Lett.* 205:179–184.
23. Dimitrov, D. S., and A. E. Sowers. 1990. Membrane electroporation—fast molecular exchange by electroosmosis. *Biochim. Biophys. Acta*. 1022:381–392.
24. Chernomordik, L. V., S. I. Sukharev, S. V. Popov, V. F. Pastushenko, A. V. Sokirko, I. G. Abidor, and Y. A. Chizmadzhev. 1987. The electrical breakdown of cell and lipid membranes: the similarity of phenomenologies. *Biochim. Biophys. Acta*. 902:360–373.
25. Kinoshita, K., and T. Y. Tsong. 1977. Voltage induced pore formation and hemolysis of human erythrocytes. *Biochim. Biophys. Acta*. 471:227–242.
26. El-Mashak, M. E., and T. Y. Tsong. 1985. Ion selectivity of temperature-induced and electric field-induced pores in dipalmitoylphosphatidyl choline vesicles. *Biochemistry*. 24:410–418.
27. Schwan, H. P. 1983. Biophysics of the interaction of electromagnetic energy with cells and membranes. In *Biological Effects and Dosimetry of Nonionizing Radiation*. M. Grandolfo, S. M. Michaelson, and A. Rindi, editors. Plenum Press, New York, 213–231.
28. Schwan, H. P. 1989. Dielectrophoresis and rotation of cells. In *Electroporation and Electrofusion in Cell Biology*. Plenum Press, New York. 3–21.
29. Yeh, C.-J. G., B.-L. Hsi, and W. P. Faulk. 1981. Propidium iodide as a nuclear marker in immunofluorescence II. Use with cellular identification and viability studies. *J. Immunol. Methods*. 43:269–275.
30. Marszalek, P., J. J. Zielinski, and M. Fikus. 1989. Experimental verification of a theoretical treatment of the mechanism of dielectrophoresis. *Bioelectrochem. Bioenerg.* 22:289–298.
31. Mehrle, W., U. Zimmermann, and R. Hampp. 1985. Evidence for asymmetrical uptake of fluorescent dyes through electroporated membranes of *Avena mesophyll* protoplasts. *FEBS (Fed. Eur. Biochem. Soc.) Lett.* 185:89–94.
32. Sowers, A. E. 1988. Fusion events and nonfusion contents mixing events induced in erythrocyte ghosts by an electric pulse. *Biophys. J.* 54:619–626.
33. Rossignol, D. P., G. L. Decker, W. J. Lennarz, T. Y. Tsong, and J. Teissie. 1983. Induction of calcium-dependent, localized cortical granule breakdown in sea urchin eggs by voltage pulsation. *Biochim. Biophys. Acta*. 763:346–355.
34. Bartoletti, D. C., G. I. Harrison, and J. C. Weaver. 1989. The number of molecules taken up by electroporated cells: quantitative determination. *FEBS (Fed. Eur. Biochem. Soc.) Lett.* 256:4–10.